Wind and Structures, *Vol. 22, No. 1 (2016) 43-63*
DOI: http://dx.doi.org/10.12989/was.2016.22.1.043

Aerostatic load on the deck of cable-stayed bridge in erection stage under skew wind

Shaopeng Li[1a], Mingshui Li[*1,2], Jiadong Zeng[1b] and Haili Liao[1,2c]

[1]*Research Centre for Wind Engineering, Southwest Jiaotong University, Chengdu,Sichuan610031, China*
[2]*Key Laboratory for Wind Engineering of Sichuan Province, Chengdu, Sichuan 610031, China*

(Received April 1, 2015, Revised October 14, 2015, Accepted October 20, 2015)

Abstract. In conventional buffeting theory, it is assumed that the aerostatic coefficients along a bridge deck follow the strip assumption. The validity of this assumption is suspect for a cable-stayed bridge in the construction stages, due to the effect of significant aerodynamic interference from the pylon. This situation may be aggravated in skew winds. Therefore, the most adverse buffeting usually occurs when the wind is not normal to bridge axis, which indicates the invalidity of the traditional "cosine rule". In order to refine the studies of static wind load on the deck of cable-stayed bridge under skew wind during its most adverse construction stage, a full bridge 'aero-stiff' model technique was used to identify the aerostatic loads on each deck segment, in smooth oncoming flow, with various yaw angles. The results show that the shelter effect of the pylon may not be ignored, and can amplify the aerostatic loading on the bridge deck under skew winds (10º-30º) with certain wind attack angles, and consequently results in the "cosine rule" becoming invalid for the buffeting estimation of cable-stayed bridge during erection for these wind directions.

Keywords: aero-static coefficients; skew wind; shelter effect; cosine rule; full aero-stiff model; CFD simulation; cable-stayed bridge

1. Introduction

The balanced cantilever method is widely used for the construction of cable-stayed bridges. It is known to be an extremely flexible structural system susceptible to wind actions for its lack of overall stiffness. Generally, auxiliary pier or wind cables are used to prevent excessive buffeting responses induced by occasional storms. Traditionally, the effects of wind yaw angle are usually ignored with an assumption that wind normal to the bridge axis should be the worst case in estimating buffeting response and designing these auxiliary structures. However, the natural wind field is stochastic both in its magnitude and in its direction, which means that the strong wind does not always have the highest probability of occurrence from the directions normal to the bridge axis. Therefore, it may be possible to exceed the ultimate stress level when a bridge is in a skew wind. Furthermore, a large number of investigations, including theoretical studies, wind tunnel tests and

∗Corresponding author, Professor, E-mail: lms_rcwe@126.com
[a] Ph.D. Student, E-mail: lishaopeng0314@163.com
[b] Ph.D. Student, E-mail: zjd_rcwe@126.com
[c] Professor, E-mail: hlliao@swjtu.edu.cn

http://www.techno-press.org/?journal=was&subpage=8 ISSN: 1226-6116 (Print), 1598-6225 (Online)

field measurements, indicated that the buffeting response of cable-stayed bridge in an erection stage with a skew wind may exceed those under a normal wind, thus indicating the limitation of the assumption mentioned above.

In the early 1950's, Scruton (1951) studied the response of a full suspension bridge model under skew wind in smooth flow. The critical wind speeds for vertical and torsional induced oscillations were observed to be higher when the wind was inclined to normal direction. Davenport *et al*. (1969a) conducted a full aeroelastic model test to investigate the response of a suspension bridge under skew wind. For the completed bridge, it was observed that the vertical buffeting response was considerably smaller under skew wind. However, for some erection stages, the response did not decrease as much with increase of wind yaw angle. In lower turbulent flow, the response has shown even less sensitivity to wind yaw angles. A concrete bridge model in completed stage was also examined by Davenport *et al*. (1969b) to study the vertical and lateral bending response under skew wind and a similar phenomenon was observed. Davenport *et al.* (1976) conducted a taut strip model test to study the peak torsional response affected by skew wind. It was observed that the torsional response had obvious sensitivity to wind direction. The response at yaw angle 20° was about a half of that under normal wind. Melbourne (1980) conducted a full model test for a cable-stayed bridge to study the effect of yaw angle. The peak vertical displacement was found to be proportional to the cosine component of wind yaw angle measured from the normal to the bridge axis.

Tanaka and Davenport (1982) proposed the so-called "cosine rule", skew wind decomposition method, to predict the buffeting response of a structure under skew wind in the frequency domain. The effect of yaw angle was fairly well represented by taking the cosine component as representative wind speed when the flow is relatively smooth. However, Zan's (1987), and Gamble and Irwin's (1985) experimental studies indicated that this approach may underestimate the actual response of a cable-stayed bridge in an erection stage under skew wind for highly turbulent wind.

By introducing the concept of effective mean wind speed, deck width, and turbulence correlation length, an approximate theory was proposed by Xie and Tanaka (1991) to estimate the buffeting response of bridge with a free end under skew wind. The turbulent component along bridge deck was ignored, and the aerodynamic influence of effective width of deck was accounted for by the ratio of effective width to integral length scale of turbulence. They assumed that the correlation of turbulence has same shape in every direction but its length scale changes following an elliptical shape. Theoretically, this approach is still a two-dimensional aerodynamic analysis, which is acceptable only if the yaw angle is not too large. However, if the bridge has unsupported free ends, the effect of three-dimensionality of structure needs to be taken into consideration. The conventional buffeting analysis was modified by Kimura and Tanaka (1992) to predict the response of a cantilever structure under a skew wind. The wind velocity was decomposed into a cosine component normal to bridge axis and a sine component parallel to bridge deck axis. The response was calculated separately corresponding to each effective wind velocity. By introducing six aerodynamic coefficients, a similar approach was applied by Scanlan (1993) to predict the response of cable-stayed bridge during erection stages to skew wind.

Zhu (2002) proposed a modified buffeting analysis method to predict the response of a bridge under skew wind by introducing a concept of oblique strip along mean wind direction. Contrary to the previous decomposition method ("cosine rule"), this approach was based on a wind coordinate system, and required a series of wind tunnel tests to obtain aerodynamic coefficients, aerodynamic admittance and flutter derivatives along the oblique strips. In order to measure the aerodynamic coefficients on an oblique sectional model, Zhu *et al.* (2002a) developed a test rig and a

measurement system. Zhu *et al.* (2002b) also proposed a dynamic test system to measure eight flutter derivatives of a typical strip of Tsing Ma bridge deck under skew winds. Based on measured parameters of Typhoon Sam and oblique sectional model, the buffeting response of Tsing Ma suspension bridge was predicted by this approach, resulting in good agreement with the measured results (Xu and Zhu 2005). Zhu *et al.* (2007) conducted a full model test of cable-stayed bridge under skew wind and found that most unfavorable buffeting responses often occurred within the yaw angle range of 5º-30º. Li *et al.* (2013) proposed an accurate cross-spectral density of wind fluctuations and developed a coherence model of buffeting force under skew winds; the traditional buffeting analysis approach could then be conveniently employed, decomposing the skew wind into a body coordinate system.

All the analytical methods mentioned above assumed that the aerostatic coefficients along a bridge deck were constant and that the strip assumption can be applied to calculate the total buffeting forces along span. However, for a cable-stayed bridge in an erection stage, the flow field, especially on the leeward side, may be modified by the bridge pylon more significantly as the wind is inclined to the normal direction. Thus, the wind load acting on the bridge deck may not be constant, but may depend on the location away from pylon. The aerostatic coefficients obtained from sectional model tests thus cannot confidently be used directly to estimate the response of a bridge under skew winds. Therefore, it is necessary to study the mechanism of the shelter effect of the pylon on the distribution of wind loading on a bridge deck under skew winds, and the relation be determined between static coefficients measured by conventional sectional model testing, and those considering the shelter effect.

In this paper, we focus on determination of the static wind loading at arbitrary locations along the deck of a cable-stayed bridge under skew winds in an erection stage, especially studying the shelter effect of the pylon. A rigid model of a cable-stayed bridge during the double cantilever erection stage was designed to identify the aerostatic loading on the deck segments. To investigate the effect of wind direction and pylon on aerostatic loads, the yaw angle was varied from -90° to 90°.

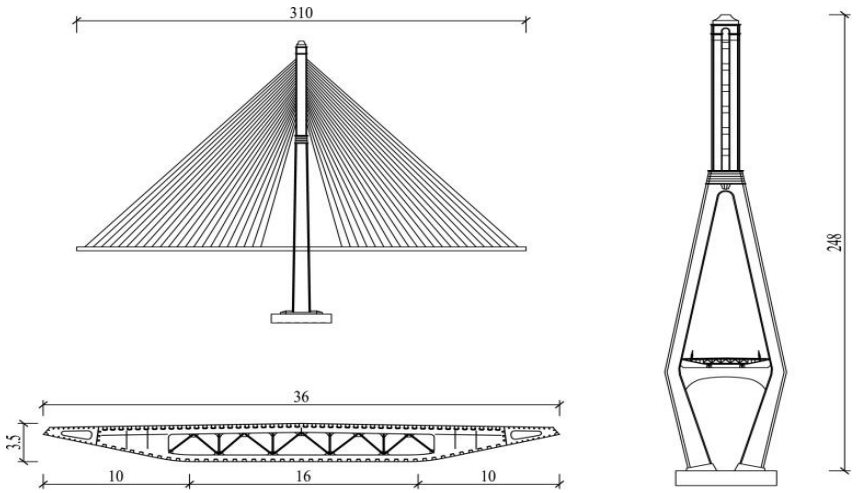

Fig. 1 General view of the cable-stayed bridge during the balanced cantilever erection stage

In addition, the effect of the attack angle of wind was also studied. The error margin of "cosine rule" was estimated by comparing the measured results with the ones obtained from a conventional section model test. Furthermore, in order to demonstrate the pylon's shelter effect, a CFD simulation was carried out to study the flow field around pylon area, to understand the invalidity of the traditional "cosine rule".

2. Engineering background

A symmetrical cable-stayed bridge in an erection stage, as shown in Fig. 1, was used. The cantilevered length of the bridge deck is 155 m long. The double-plane cable system uses a fan-type cable arrangement. The steel streamlined box girder is 36.0m in width and 3.5 m in depth. The concrete pylon, with a diamond shape, is 248 m high.

The static wind load on bridge deck was measured by a series of wind tunnel tests, including a section model test, and a full 'aero-stiff' model test, conducted at Research Center for Wind Engineering of Southwest Jiaotong University, Chengdu. The object of these tests was to investigate the spatial distribution of static wind loading on bridge deck under a skew wind, especially the shelter effect of a pylon.

3. Experimental technique

3.1 Sectional model test

Traditionally, the aerostatic coefficients of a bridge deck are measured in smooth approach flow by a section model test as shown in Fig. 2. In this case, a geometric scaling ratio of 1:50 was chosen for the design and manufacture the section model. The length of this model (L) was 2.095 m, the width (B) was 0.720 m and the depth (H) was 0.070 m. The sectional model was designed and manufactured using conventional stiff model technology, using high quality light wood and plastic. The wind tunnel (XNJD-1) of Southwest Jiaotong University, a closed circuit wind tunnel, with two tandem closed test sections, was used to carry out the tests. The dimension of the test section for sectional model test is 2.4 m×2.0 m×16.0 m (W×H×L), with the wind speed adjustable from 1 m/s to 45 m/s (turbulent intensity<0.5%). A balance system, mounted on outside of the wind tunnel, was used in this investigation.

The static wind load acting on bridge deck can be defined in a body coordinate system, as shown in Fig. 3.

The drag and lift coefficients are defined as

$$C_D(\alpha) = F_D(\alpha) \Big/ \left(\frac{1}{2} \rho U^2 HL \right) \tag{1}$$

$$C_L(\alpha) = F_L(\alpha) \Big/ \left(\frac{1}{2} \rho U^2 BL \right) \tag{2}$$

Fig. 2 View of traditional section model test in XNJD-1 wind tunnel

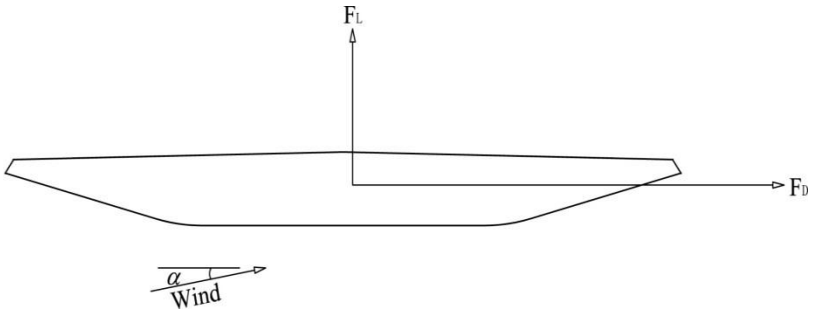

Fig. 3 Definition of wind load and coordinate system

Table 1 The aerostatic coefficients

α(°)	C_D	C_L
1.5	0.6924	0.1720
-1.5	0.4649	-0.2513
-4.5	0.1995	-0.5135

α is the attack angle of wind, with the positive angle shown in Fig. 3. U is the wind speed, ρ is the air density. B, H and L are width, height and length of the sectional model, respectively. $F_D(\alpha)$, $F_L(\alpha)$ are drag and lift acting on the deck in body coordinate system.

The measured aerostatic coefficients, corresponding to effective attack angle of the full aero-stiff model during wind tunnel testing, are listed in Table 1.

3.2 Full 'aero-stiff' model test

The traditional sectional model test described in Section 3.1 cannot represent the three-dimensionality of the flow field affected by the pylon. In place of an aero-elastic model test, a full 'aero-stiff ' model was conceived to study the shelter effect of the pylon (see Fig. 4).

The full 'aero-stiff' model of cable-stayed bridge in the erection stage (see Fig. 4(a)), with a geometric scale of 1:70, was constructed. Compared with an aero-elastic model, the full aero-stiff model has sufficiently high stiffness and remains stationary under high-speed wind. This approach makes it possible to measure the aerostatic forces on each segment by a force balance attached to the spine structure.

The metal spine assembly of main girder was designed as a rectangular steel beam with high stiffness. External elements of the girder were made of fibre-glass and ABS (Acrylonitrile Butadiene Styrene) material. To avoid interference between two adjacent sections, a 3mm gap between sections was included.

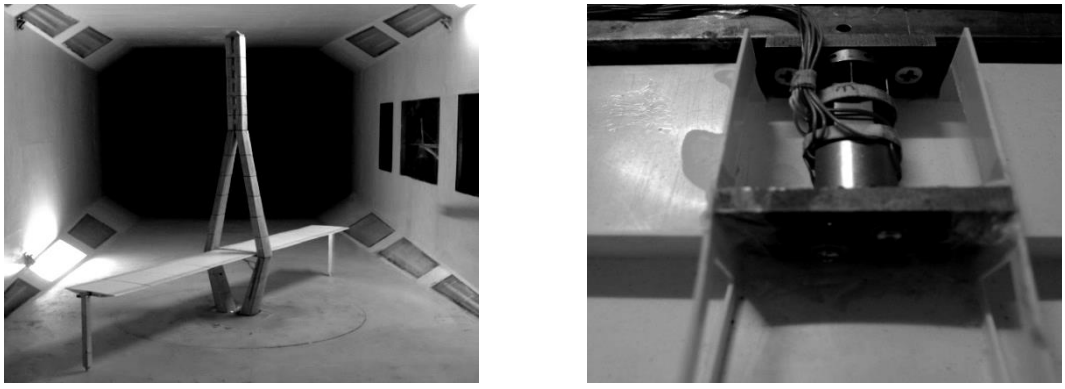

(a) Full 'aero-stiff' model (b) Force balance system

Fig. 4 Schematic diagram of full 'aero-stiff' model and force balance system

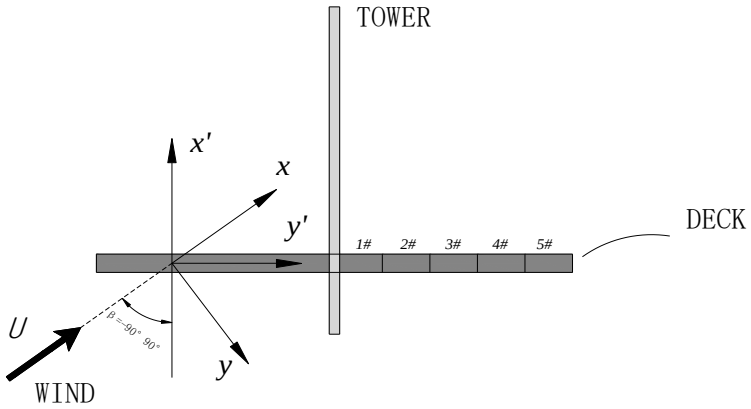

Fig. 5 Deck segments and definition of coordinate systems

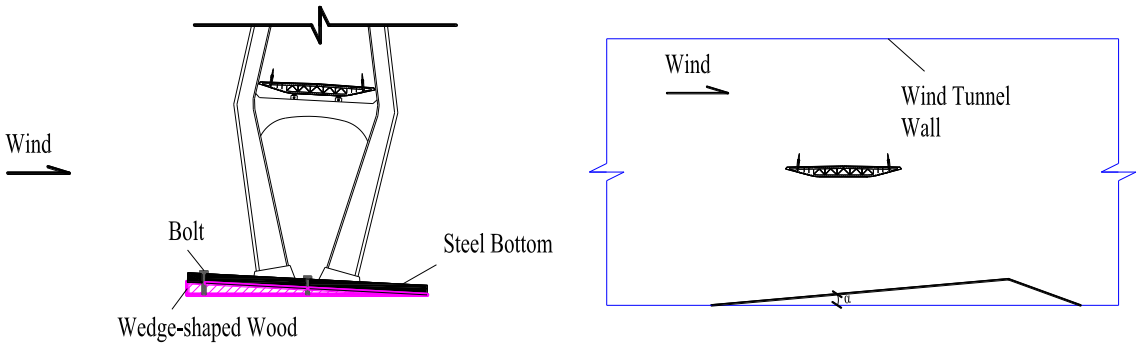

(a) 'Overall-model booster' method (b) 'Attack-angle panel' method

Fig. 6 The device for changing attack angle

Five sets of balance systems were used to measure the forces on all the sections simultaneously. Balances with a load range of 10N were used in these tests. They were fixed to the metal spine, and the segments of girder were connected with the balances directly (see Fig. 4(b)). Prior to the experiments, the balances were calibrated by applying a series of loads for lift and drag forces directly. The results show that these balances were of high accuracy with the relative error of less than 0.5%. Then the drag force, axis force and lift force on each element induced by wind could be measured in body coordinates. As shown in Fig. 5, the static wind loads on five sections were measured, with wind yaw angle varying from -90° to 90°. The 0° yaw angle is defined as the wind normal to the bridge deck axis, and the yaw angle of 90° is defined with the measured segments located upstream; at the yaw angle of -90° these are located downstream.

Usually, full bridge aeroelastic model wind tunnel tests can only be conducted under a 0° wind attack angle in the vertical plane. However, if the aerodynamic characteristics of structures under other attack angles need to be measured, several immature simulation methods can be used (Sun *et al*. 2013), including the 'overall-model booster' method (see Fig. 6(a)). and the 'attack-angle panel simulation' method (see Fig. 6(b)).

The 'overall-model booster' method makes use of a wedge to incline the overall model ar the base; then a certain attack angle acting on the test model is created to achieve the required attack angle. The 'attack-angle panel' simulation method requires a trapezoidal plate of a certain height, depending on the height of bridge site, so that a flow field of certain angle is generated when the wind passes through the plate.

However, both simulation methods have some unavoidable flaws. The 'overall-model booster' method is simple, but this method will change the relative direction of gravity, and the damping ratio is hard to determine when the aero-elastic model is transformed into other angle of attack. The 'attack-angle panel' method requires different attack angle simulation equipment under different conditions, depending on the height of bridge site, and other disadvantages such as time-consumption, cost, and the change of the flow field in turbulent flow should also be taken into consideration.

For convenience, the 'overall-model booster' method was adapted to the aero-elastic model wind tunnel tests, and a wedge-shaped wood with certain angle was installed at the base of the full aero-stiff model to change the angle of attack of the wind. Taking the deformation of the model into consideration, the aerostatic wind loading on bridge deck, with effective attack angles of

+1.5º,-1.5º and -4.5º during the tests , was measured.

The full 'aero-stiff' model test was carried out in an industrial wind tunnel (type: XNJD-1) at Southwest Jiaotong University. The first test section, 3.6 m(B) × 3.0 m(H) × 8.0 m(L), was used in this investigation. The wind speed is adjustable from 0.5 m/s to 22.0 m/s. The aerostatic loads on deck segments were investigated in smooth flow with a wind velocity U=15 m/s.

4. Experimental results and discussions

4.1 Distribution of the static wind loads from full aero-stiff model tests

The distribution of the static wind load on the girder with wind velocity normal to the bridge deck axis was investigated. Fig. 7 shows the variation of lift coefficients on each deck segment. Compared with the results obtained from section model test, the static lift loads acting on the bridge deck segments are not constant as shown in Fig. 7(a). However, the lift on segments farther away from pylon was consistent with the section model test; this validates this experimental technique. It was also observed that a region in which amplification of the lift acting on bridge deck exists, caused by the shelter effect of the pylon; this is about 1/5 pylon heights away from the pylon. This tendency became more obvious as the attack angle increased to positive as shown in Fig. 7(b), which indicated that the shelter effect may be related to the wind incident angle. The reduction of lift on segment 5# was expected due to the possible three-dimensional flow influence at the tip of bridge deck. These results may imply that the uniform flow was disturbed dramatically while it approaching the pylon. Thus, a compressed and distorted flow was formed around the pylon area, causing the static wind load acting on bridge deck near this region to be amplified significantly.

The sectional static coefficients of lift and drag force, varying with the location along bridge deck, and with the wind direction, are shown in Fig. 8. The drag load reached a maximum under skew winds due to the pylon shelter effect (see Figs. 8(a)-8(c)). A similar tendency is also observed for lift as shown in Figs. 8(d)-8(f). In addition, it is also seen that the occurrence of maximum wind loads under skew wind is related to the attack angle; this may enhance the shelter effect of the pylon.

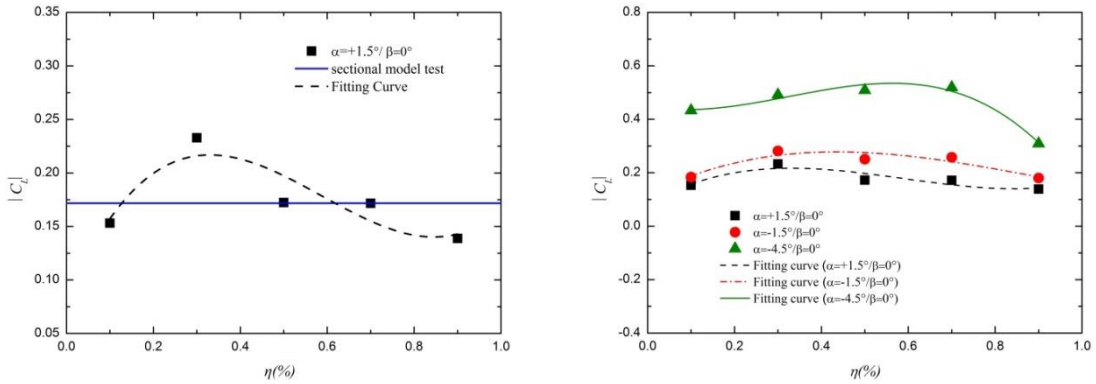

(a) Sectional model test & aero-stiff model test (b) Lift distribution varying with attack angle

Fig. 7 Influence of wind incident angle and pylon on the distribution sectional lift

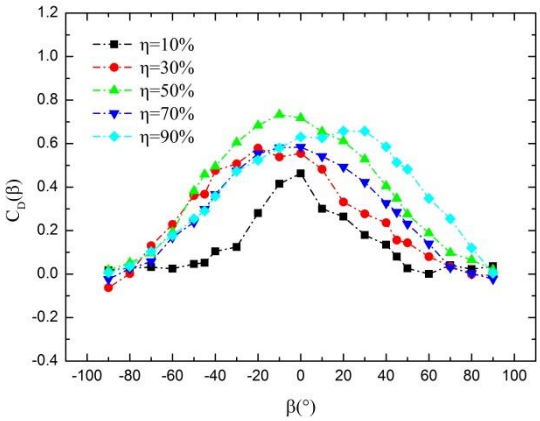

(a) Drag coefficients (α=+1.5º)

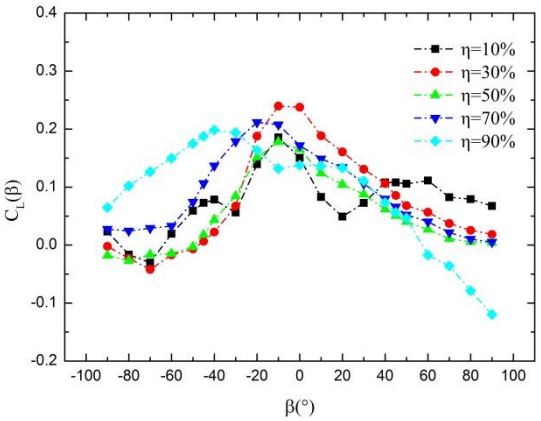

(d) Lift coefficients (α=+1.5º)

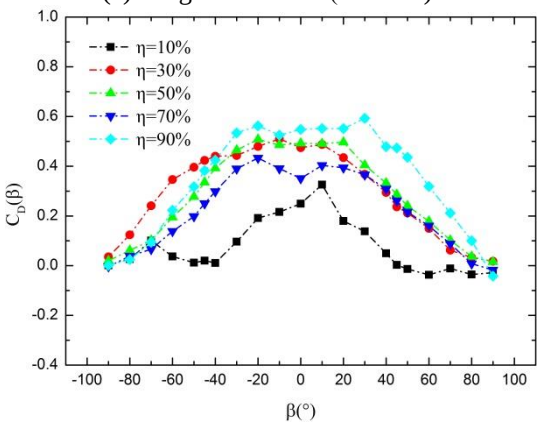

(b) Drag coefficients (α=-1.5º)

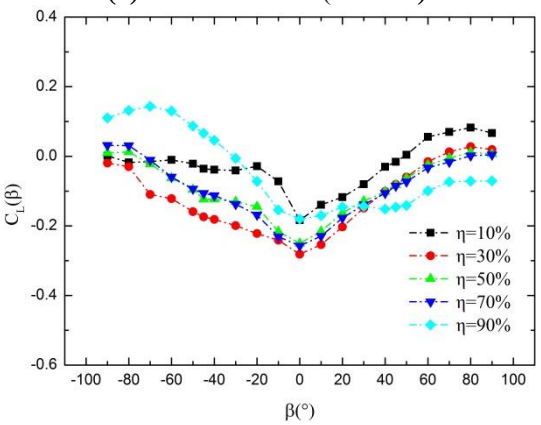

(e) Lift coefficients (α=-1.5º)

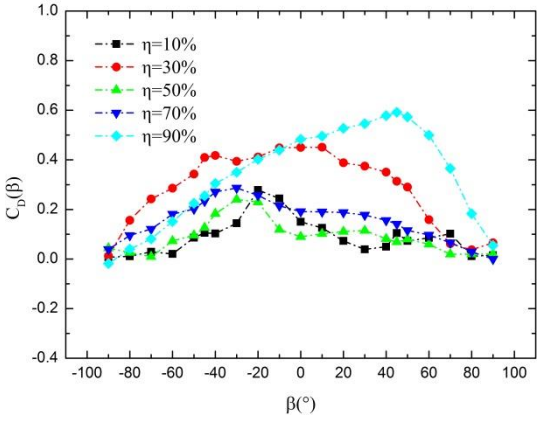

(c) Drag coefficients (α=-4.5º)

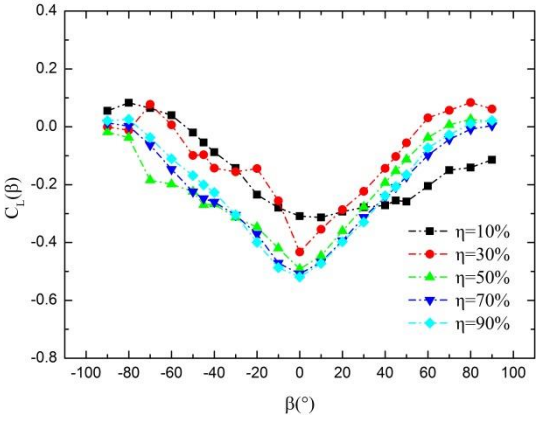

(f) Lift coefficients (α=-4.5º)

Fig. 8 Static coefficients varying with location and wind direction

The "cosine rule", proposed by Liu *et al.* (2008), can be written as

$$\cos^2(\beta) = \frac{C_i(\alpha,\beta)}{C_i(\alpha,0)} \tag{3}$$

where β is yaw angle; α is attack angle; $C_i(\alpha,\beta)$ is the aerostatic coefficient; *i* represents drag coefficient (*D*) and lift coefficient (*L*).

Based on the measured results, the error margin of the "cosine rule" is shown in Fig. 9. For a cable-stayed bridge in a balanced cantilever erection stage, the aerostatic wind loads on main girder are not only related to the yaw angle, but also to the wind attack angle and location along the bridge deck. As shown in Fig. 9(a), the variation of drag force varying with yaw angle is generally consistent with the "cosine rule" when the wind incident angle is positive. However, for leeward segments near the pylon, the most disadvantageous drag load appears at a yaw angle of 20°, indicating that the shelter effect of the pylon only influences smaller regions behind the pylon for positive attack angles. Compared with Fig. 9(a), Figs. 9(b)-9(c) indicates that the "cosine rule" is invalid for drag forces at negative attack angles. For the windward segment near the pylon (1#), the static drag load approached the "cosine rule" for negative attack angle. However, for windward segments relatively far away from the pylon (3#-4#), the drag loads reach a maximum when the yaw angle is around 10°-20°. For the leeward segments, the most severe drag load occurs as the yaw angles approach -20° to -30°; this is enhanced with a large negative attack angle.

In contrast, the lift approximately agrees with "cosine rule" when the wind incident angle is negative as shown in Figs. 9(e)-9(f). With respect to positive incident angles, only the windward segments approximately matched the "cosine rule" as shown in Fig. 9(d). However, for the leeward segments farther away from pylon, the lift reached its maximum when the yaw angle was about 20°. With regard to the leeward segments near the pylon, the maximum lift appeared at yaw angle approaching 10°, and decreased more rapidly with increasing of yaw angle compared with traditional "cosine rule". The results indicated that the pylon influenced the distribution of lift on leeward segments more significantly, when the wind incident angle became positive, and the shelter effect of the pylon attenuated for the negative incident angle of the wind, and consequently the traditional "cosine rule" could be applied approximately to predict the response of a bridge under skew winds.

A possible explanation is that that the shelter effect changes the flow field, and generates a complex vortex around the pylon; this may significantly affect the surface pressure distribution at some points along the bridge deck. When the wind incident angle is positive, the shelter effect of the pylon mainly influences the lift on leeward segments relatively far away from the pylon obviously. In contrast, the shelter effect significantly influences the drag load on the free ends of the girder for negative attack angles.

In summary, the shelter effect of the pylon on lift loading will obviously be amplified when the wind attack angle is positive, and the lift coefficient of bridge girder behind pylon reaches a maximum as the wind deviates 10°-20° from the normal direction. The most adverse drag loading appears for a skew wind (10°-30°) with negative attack angle.

4.2 Flow field around the pylon

In order to demonstrate the characteristics of flow field disturbed by the pylon under skew winds, a CFD simulation was carried out to visualize the flow field around the pylon when the yaw

angle was 15°. The lift coefficients of the leeward segments obtained by CFD were compared with those from the full 'aero-stiff' model test to validate the simulated results.

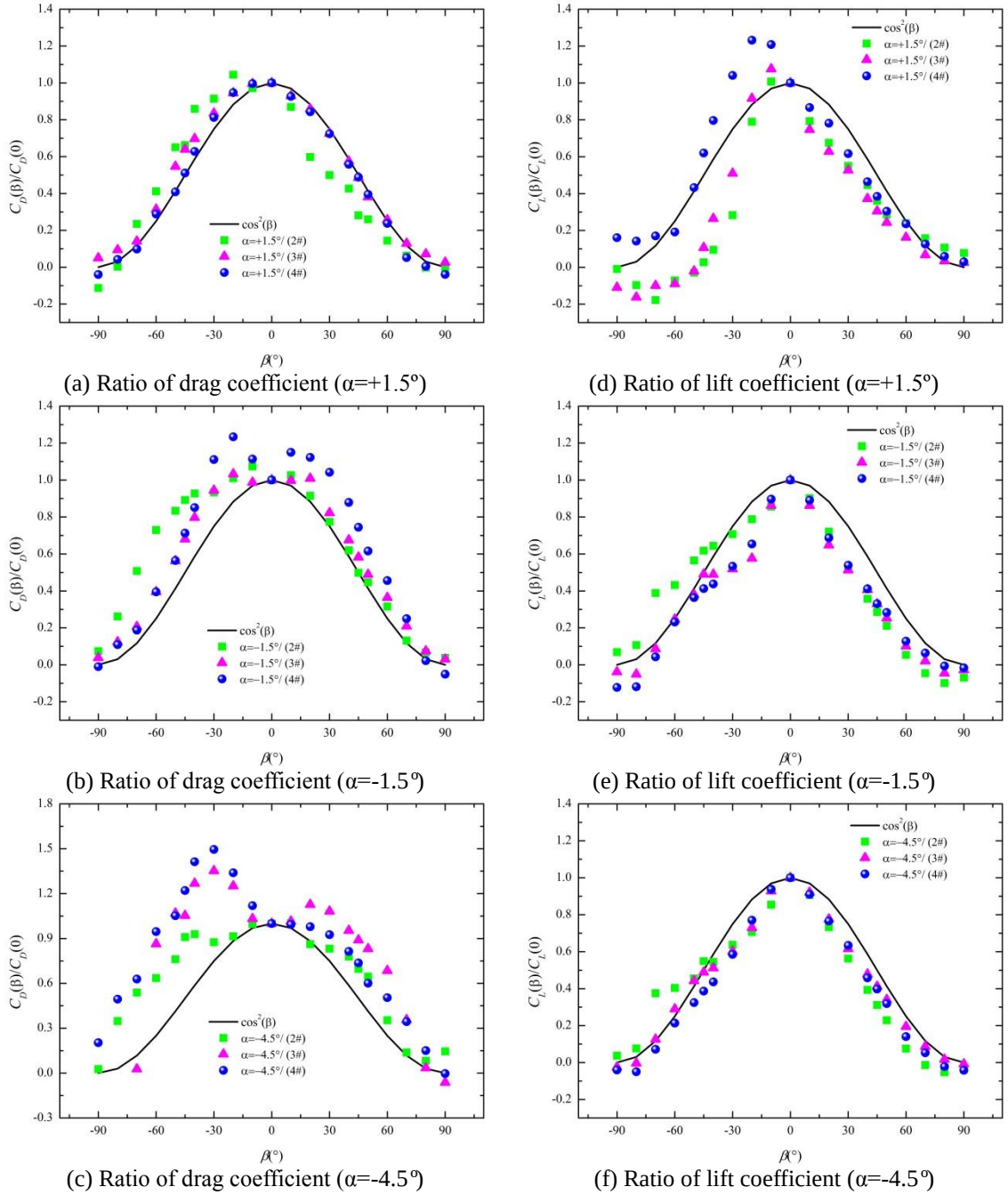

(a) Ratio of drag coefficient (α=+1.5°) (d) Ratio of lift coefficient (α=+1.5°)

(b) Ratio of drag coefficient (α=-1.5°) (e) Ratio of lift coefficient (α=-1.5°)

(c) Ratio of drag coefficient (α=-4.5°) (f) Ratio of lift coefficient (α=-4.5°)

Fig. 9 Error margin of the "cosine rule"

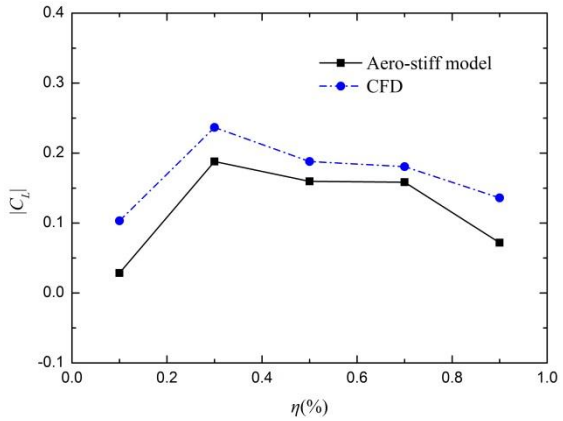

Fig. 10 Comparison of $|C_L|$ on leeward segments obtained by CFD and by the full 'aero-stiff' model test (β=15º)

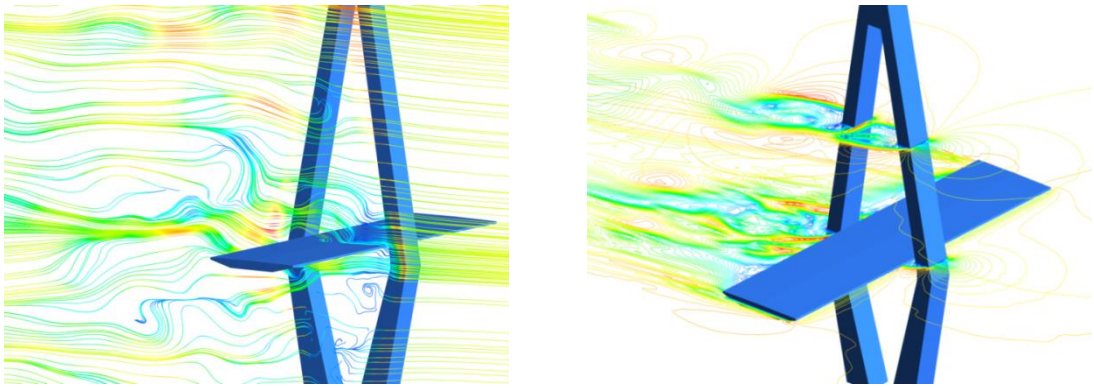

(a) The streamline near pylon area (β=15º) (b) The velocity field near pylon area (β=15º)

Fig. 11 The flow field near pylon area simulated by CFD (β=15º)

Fig. 10 shows that the results obtained by CFD are larger than those by wind tunnel test, but the tendency of two results is consistent, which indicates that the following CFD simulation is reliable. Then, as shown in Fig. 11(a), it is observed that the streamline is distorted dramatically by the pylon. Explicit vortex emerging behind the pylon in a certain spatial region could be observed, which may dramatically influenced the wind loading distribution along the bridge deck. The variations of velocity field due to the pylon's shelter effect are also simulated as shown in Fig. 11(b). It is found that the velocity in a smaller region on the windward deck near the pylon is also distorted. When smooth flow passing through the pylon, the velocity field in a considerable region behind pylon is dramatically affected, and then a certain velocity amplification region behind the pylon is formed obviously, which may present a qualitative explanation to the mechanism of wind loading amplification for leeward girder due to pylon's shelter effect.

5. Numerical example

Based on the measured results, the response of a cable-stayed bridge in cantilever erection stage was calculated to study the error margin caused by the shelter effect of the pylon.

The geometrical dimensions of the cable-stayed bridge were consistent with the previous one described in Section 2. Static responses of the most adverse section of girder were obtained by the Finite Element Method (FEM) as shown in Fig. 12. The static responses, including displacement at free end of the girder (lateral displacement d_x along the x axis, vertical displacement d_z along the z axis) and internal forces (shear force F_x and F_z, moment M_z and M_x) at the joint section of the pylon and girder, as shown in Fig. 13, were calculated. The mean wind speed used for the following analysis was 32 m/s. For evaluation of the structural response of classic cable-stayed bridge at maximum cantilever erection stage under skew wind and the shelter effect of the pylon, three cases were considered:

(a) Static loading measured from sectional model tests and application of "cosine rule", - defined as Case 1#;

(b) Static loading measured from full aero-stiff model tests with yaw angle β=0º and application of "cosine rule" - defined as Case 2#;

(c) Static loading measured from full aero-stiff model tests varying with yaw angles (actual static wind loading) - defined as Case 3#.

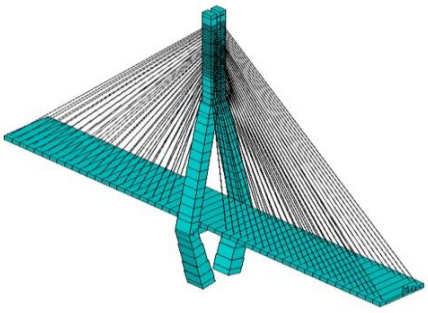

Fig. 12 Finite element model

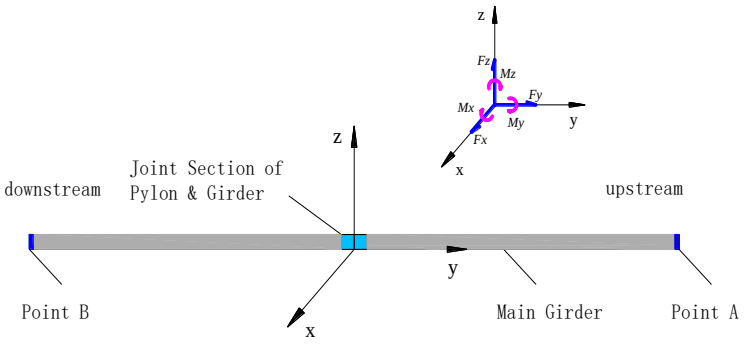

Fig. 13 Coordinate system

5.1 Structural displacement under static wind loading

It should be noted that the drag and lift loads acting on bridge deck were considered separately when calculating the corresponding structural response, including the displacements at the free ends of the main girder, and the internal forces at the joint section between the pylon and girder.

The lateral displacements d_x at both end of girder, with only drag loading acting on the girder, are shown in Fig. 14. Comparing Fig. 14(a) with Fig. 14(d), it is obvious that the traditional sectional tests and "cosine rule", are found to be somewhat conservative with respect to the results based on full aero-stiff model tests, when the attack angle is positive. In addition, the results indicated that the normal wind direction is the most disadvantageous condition for drag loading. When the attack angle is -1.5°, the sectional model tests and "cosine rule" are also effective under normal wind condition as shown in Figs. 14(b) and 14(e). However, Case 1# and Case 2# underestimate the static wind loading under skew winds and could potentially introduce risk in the construction stage. In spite of this, the method proposed as Case 1# is still available if the structural loading is designed based on the normal wind condition, whereas Case 2# was proved to be invalid. For the negative incident angles between 0° and -4.5°, as in Figs. 14(c) and 14(f), Cases1# and 2# indicate a risk of overturning and collapse of the leeward girder behind pylon. Case 3# indicates that the lateral displacement at free end of the girder in leeward reaches its maximum when the yaw angle is about 30°. However, the error margin of displacement d_x at the free ends in windward is still acceptable.

Compared with the lateral bending stiffness, the main girder provides smaller vertical bending stiffness, and is vulnerable to the asymmetric lift on the cantilevered deck. Therefore, the "cosine rule" could cause serious errors in the prediction of structural response induced by wind loading, as shown in Fig 15. For positive incident angles reaching +1.5°, Case 1# and Case 2# cannot accurately predict the vertical displacement, d_z, at the free end of the girder on both sides, as shown in Figs. 15(a) and 15(d). In addition, the maximum vertical displacement appears when the yaw angle is about 20°. When the attack angle is negative, Case 1# and Case 2# also fail to predict the vertical response of girder due to lift loading. In contrast to the positive incident angle condition, the normal wind direction is the most disadvantageous case. For negative attack angles, Figs. 15(b) and 15(e) show that the vertical displacements of girder at both sides are quite large at yaw angle 60°, requiring attention during construction. When the negative incident angle decreases to -4.5°, a similar phenomenon is observed.

The error margins of lateral and vertical displacements, as defined in Equation (4), are listed in Table 2.

$$\eta_i = \left| \frac{\left(F_i^{case3\#}\right)_{\max} - \left(F_i^{case1\#}\right)_{\max}}{\left(F_i^{case3\#}\right)_{\max}} \right| \times 100 \tag{4}$$

where $i = (d_x, d_z, F_x, F_z, M_x, M_z)$ represents the displacement and internal force defined in Fig. 13, respectively.

5.2 Structural internal force under static wind loading

The shear force and bending moment at the joint section of the pylon and girder were also calculated, as shown in Figs. 16 and 17, respectively.

Table 2 Error margin of the displacement caused by sectional model test and "cosine rule"

Parameters	d*x*	d*z*
α(°)	-4.5	+1.5
|β (°)|	30	20
η (%)	33.1	69.4

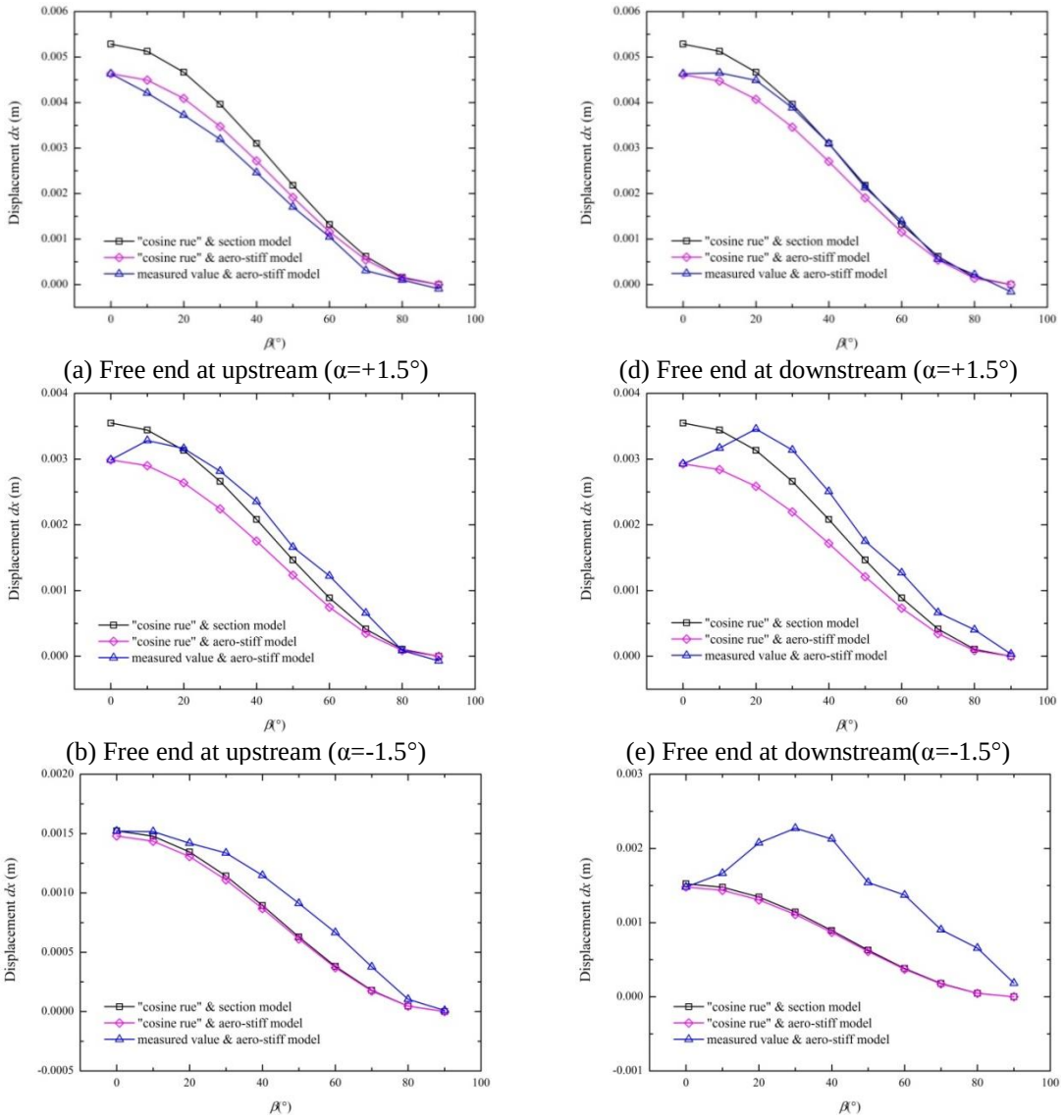

(a) Free end at upstream (α=+1.5°) (d) Free end at downstream (α=+1.5°)

(b) Free end at upstream (α=-1.5°) (e) Free end at downstream(α=-1.5°)

(c) Free end at upstream (α=-4.5°) (f) Free end at downstream(α=-4.5°)

Fig. 14 Lateral displacement (d_x) at free end of the girder

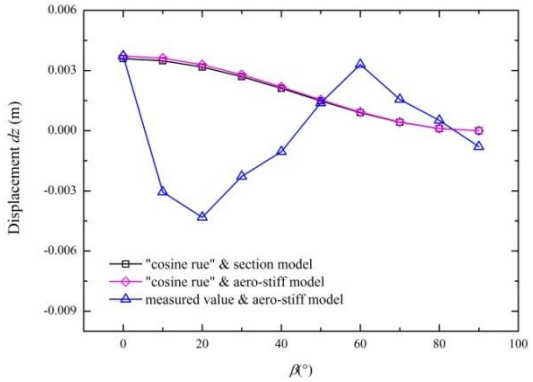

(a) Free end at upstream (α=+1.5°)

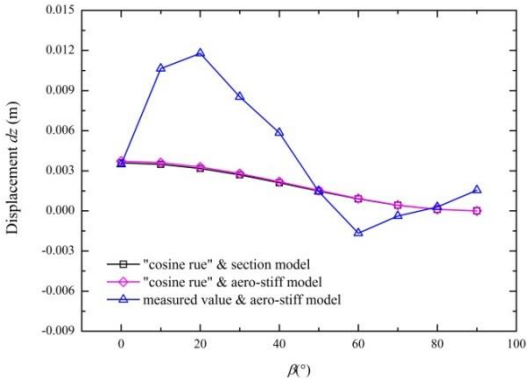

(d) Free end at downstream (α=+1.5°)

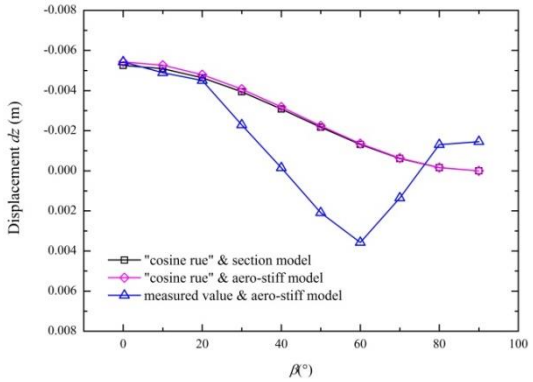

(b) Free end at upstream (α=-1.5°)

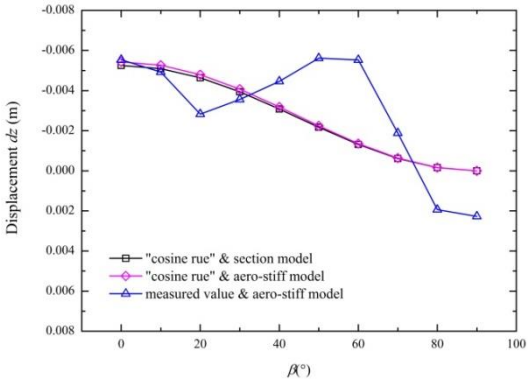

(e) Free end at downstream (α=-1.5°)

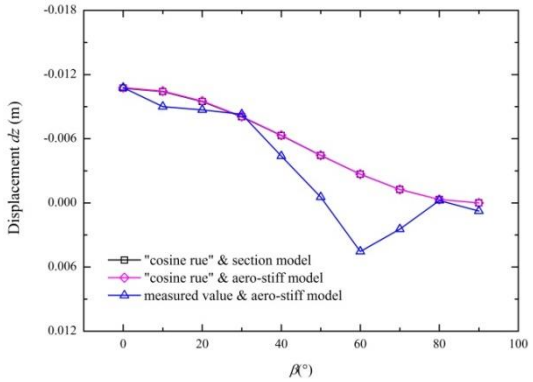

(c) Free end at upstream (α=-4.5°)

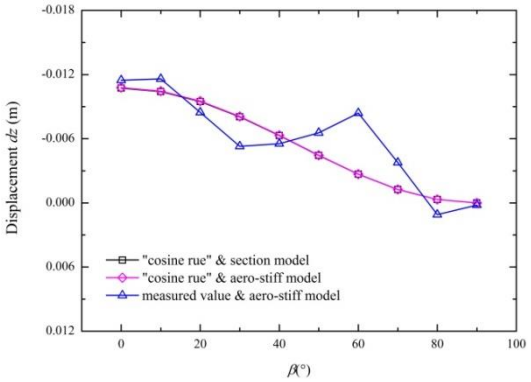

(f) Free end at downstream (α=-4.5°)

Fig. 15 Vertical displacement (d_z) at free end of the girder

For the drag loading, similar results are obtained for the three cases when incident angle is +1.5° (see Figs. 16(a) and 17(a)). The lateral shear force F_x and moment M_z reach their maximum as the wind normal to bridge deck. For negative wind incident angles, Case 1#and Case 2# seriously underestimate the structural internal force under skew wind. However, as shown in Figs. 16(b) and 17(b), the actual maximal internal force (α=-1.5°, β=20°) obtained from Case 3# is close

to the maximum results (α=-1.5º, β=0º) obtained by the traditional method (Case 1#). Thus, the section model test and "cosine rule" could be regarded as a conservative design method in this case. For larger negative attack angles (α=-4.5º), Case 1# and Case 2# failed to predict the internal force F_x and M_z (see Figs. 16(c) and 17(c)). It is seen that the maximum internal force induced by drag loading occurs when the yaw angle is about 30°. As shown in Table 3, the error margins of the traditional approach (case 1#) can reach 33.1% for F_x and 47.6% for M_z; this is unacceptable for practical design of cable-stayed bridges.

With respect to the lift action, Case 1# and Case 2# cannot accurately predict the internal force at joint section of girder and pylon when the attack angle is positive, as shown in Figs. 16(d) and 17(d). In this case, the maximal internal forces F_z and M_x are generated when the yaw angle is around10º. As shown in Table 3, the error margin of Case 1# reaches 35.4% for F_z and 43.1% for M_x, respectively; this could possibly result in a catastrophic accident during the girder installation. When the wind incident angle increases to +1.5°, the section model test and "cosine rule" can be conservatively applied, as shown in Figs. 16(e) and 17(e) for yaw angles less than 30°. However, the traditional approach is invalid when the yaw angle is larger than 30°. In addition, the most adverse yaw angle increases with larger negative attack angle; for example, it is up to 30° as the attack angle is -4.5º (see Figs. 16(f) and 17(f)).

Generally, the pylon has significant effect on internal force induced by drag loading when the wind attack angle is negative. The maximum internal force occurs when the yaw angle reaches 30°. However, the shelter effect of the pylon on lift loading will be obviously amplified when the wind incident angle is positive, and the internal force in the joint section area reaches a maximum as the yaw angle approaches 10°.

6. Conclusions

A full bridge 'aero-stiff' model has been used to investigate the spatial distribution of static wind load on the deck of cable-stayed bridge, in the balanced cantilever erection stage under skew winds. Compared with the section model test, the measured results obtained from full aero-stiff model tests indicate that the static wind loading acting on bridge deck is not constant in either normal wind or skew winds. For normal winds, an area of amplification of the static wind load is found due to the shelter effect of the pylon; the location of this region is about 1/5 pylon heights away from the pylon.

Table 3The error margin of internal force caused by sectional model test and "cosine rule"

Parameters	F*x*	F*z*	M*x*	M*z*
α(°)	-4.5	+1.5	+1.5	-4.5
|β (°)|	30	10	10	30
η (%)	33.1	35.4	43.1	47.6

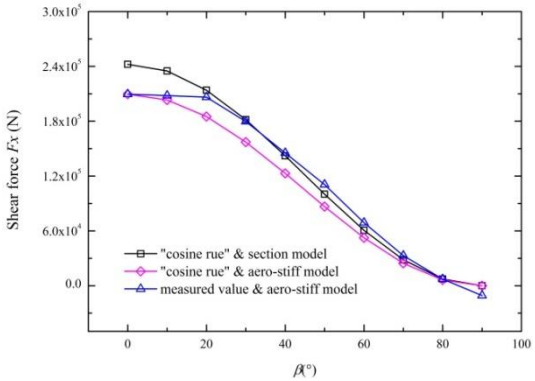

(a) Lateral shear force F_x by drag loading (α=+1.5º)

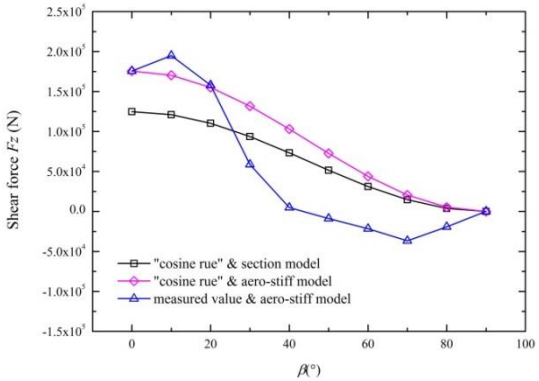

(d) Vertical shear force F_z by lift loading (α=+1.5º)

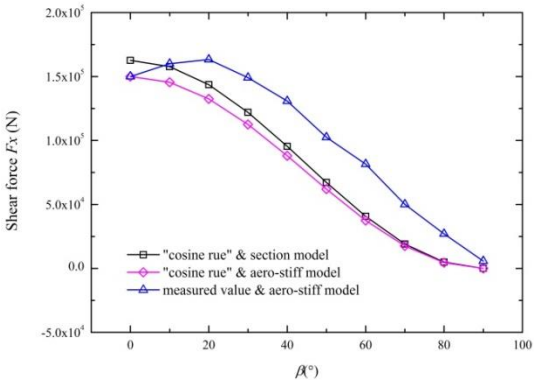

(b) Lateral shear force F_x by drag loading (α=-1.5º)

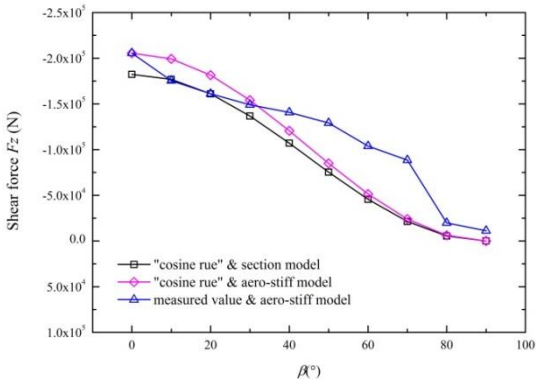

(e)Vertical shear force F_z by lift loading (α=-1.5º)

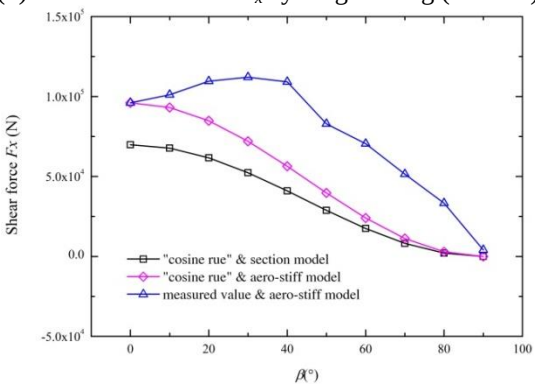

(c) Lateral shear force F_x by drag loading (α=-4.5º)

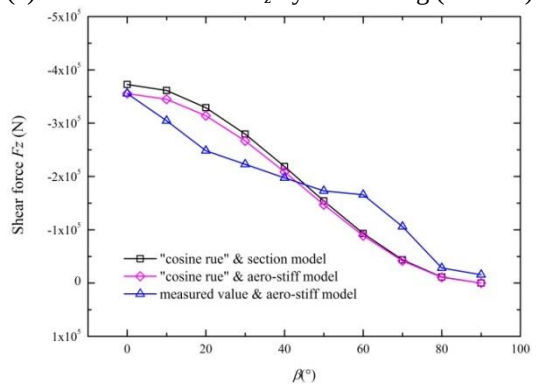

(f) Vertical shear force F_z by lift loading (α=-4.5º)

Fig. 16 Shear force at joint section of pylon and girder

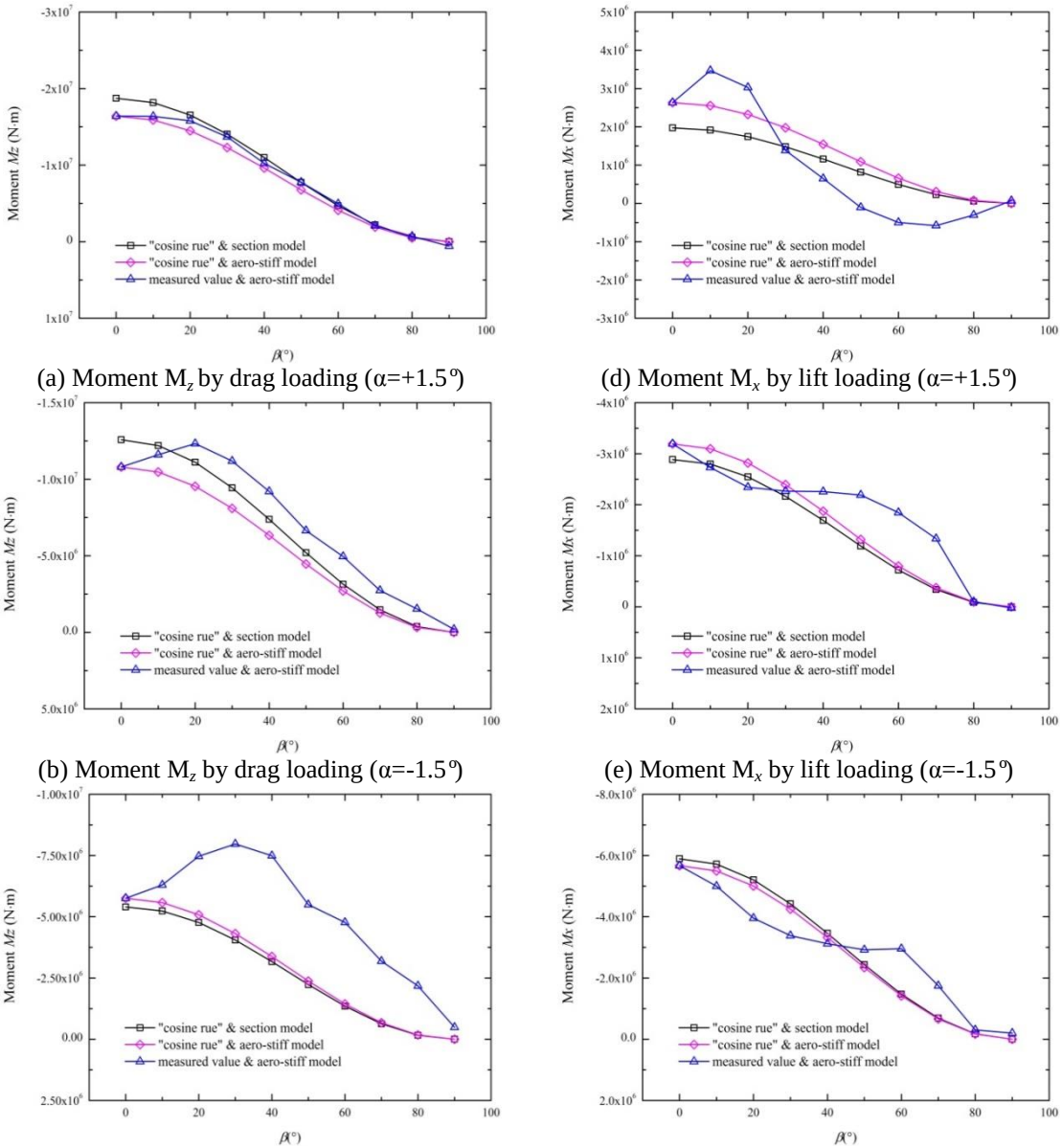

(a) Moment M_z by drag loading (α=+1.5º) (d) Moment M_x by lift loading (α=+1.5º)

(b) Moment M_z by drag loading (α=-1.5º) (e) Moment M_x by lift loading (α=-1.5º)

(c) Moment M_z by drag loading (α=-4.5º) (f) Moment $_{Mx}$ by lift loading (α=-4.5º)

Fig. 17 Moment at joint section of pylon and girder (α=-4.5º)

This tendency becomes more obvious as the wind incident angle becomes positive. For the wind direction normal to bridge deck, it is observed that the static wind loads acting on windward deck sections are inconsistent with the ones on leeward sections, which indicates that shelter effect of the pylon plays an essential role in re-shaping the surface pressure distribution on deck. Due to this effect, the most disadvantageous static wind loading may occur as the wind yaw angle varies between 10^{o} to 30^{o}. It is also obvious that the shelter effect of the pylon is sensitive to the attack angle of wind. For drag loading on the deck, the shelter effect is dramatically enhanced when the wind incident angle becomes negative. In contrast, the pylon influences the lift on bridge deck significantly as the wind incident angle becomes positive. The difference in shelter effects by the pylon for drag and lift loadings may be caused by the asymmetry of the streamlined girder and non-uniform shape of the pylon. Therefore, under special attack angle condition, the traditional "cosine rule" may be invalid as a result of the shelter effect, especially for the bridge desk segments located at leeward side. The flow field around the pylon, simulated by CFD method, further confirms that the shelter effect can seriously affect the distribution of static wind loading on the bridge deck under skew wind. The error margin of the "cosine rule" is relatively acceptable for drag loading when the wind incident angle is positive. However, the traditional approach may seriously underestimate the static wind loading for larger negative attack angles. With regard to the lift action, the traditional approach fails to predict the static response of a bridge under skew winds.

This paper only discusses a pylon with diamond shape. However, for other types of pylon, such as the H-shape, A shape or inverted Y shape, it is necessary to conduct a series of full aero-stiff model tests to verify the characteristics of static wind loading acting on the bridge deck under skew wind due to the shelter effect of the pylon.

Acknowledgments

This work is supported by the National Natural Science Foundation under the grant number 51278435, 51478402 and China National Basic Research Plan"973"under the grant number 2013CB036301.

References

Davenport, A.G., Isyumov, N., Fader, D.J. and Bowen, C.F.P. (1969a), *A study of wind action on a suspension bridge during erection and on completion: the Narrows bridge*, BLWT-3-69.

Davenport, A.G., Isyumov, N., Fader, D.J. and Bowen, C.F.P. (1969b), *An aeroelastic study of the Northumberland straits bridge-cantilevered concrete design*, BLWT-4-69.

Davenport, A.G., Isyumov, N. and Tanaka, H. (1976), *A study of wind action for the Bronx Whitestone suspension bridge*, BLWT- SS3-76.

Gamble, S.L. and Irwin, P.A. (1985), "The action of wind on a cable stayed bridge during construction", *Proceedings of the 5th US National Conference in Wind Engineering*, Lubbock, America, November.

Kimura, K. and Tanaka, H. (1992), "Bridge buffeting due to wind with yaw angles", *J. Wind Eng. Ind. Aerod.*, **42**(1-3), 1309-1320.

Li, S.P., Li, M.S. and Ma, C.M. (2013), "Buffeting analysis of long span bridge under skew wind in frequency domain", *Proceedings of the 8th Asia-Pacific Conference on Wind Engineering*, Chennai, India,

December.
Liu, X.B., Chen, Z.Q. and Liu, Z.W. (2008), "Experimental study on the aerodynamic coefficients of long span bridge deck under skew winds (in Chinese)", *J. Hunan Univ.* :*Nat. Sci. Ed.*, **35**(9), 9-14.
Melbourne, W.H. (1980), "Model and full scale response to wind action of the cable stayed box girder west gate bridge", *Proceedings of the IAHR/IUTAM Symposiums on Practical Experiences with Flow-Induced Vibrations*, Karlsruhe, Germany, September.
Scanlan, R.H. (1993), "Bridge buffeting by skew winds in erection stages". *J. Eng. Mech. - ASCE*, **119**(2), 251-269.
Scruton, C. (1951), *Experiments on the aerodynamic stability of suspension bridges*, NPL-185-199.
Sun, Y.G., Li, M.S. and Liao, H.L. (2013), "Investigation on vortex-induced vibration of a suspension bridge using section and full aeroelastic wind tunnel tests", *WindStruct*.,**17**(6), 565-587.
Tanaka, H. and Davenport, A.G. (1982), "Response of taut strip models to turbulent wind", *J. Eng. Mech. Div. - ASCE*, **108**(1), 33-49.
Xie, J. and Tanaka, H. (1991), "Buffeting analysis of long span bridges to turbulent wind with yaw angles", *J. Wind Eng. Ind. Aerod.*, **37**(1), 65-77.
Xu, Y.L. and Zhu, L.D. (2005), "Buffeting response of long-span cable-supported bridges under skew winds. Part 2: case study", *J. Sound Vib.*, **281**(3-5), 675-697.
Zan, S.J. (1987), *The effects of mass, wind angle and erection technique in the aeroelastic behavior of a cable-stayed bridge model*, NAE-AN-46.
Zhu, L.D. (2002), *Buffeting response of long span cable supported bridges under skew winds field measurement and analysis*. Ph.D. Dissertation, The Hong Kong Polytechnic University, Hong Kong.
Zhu, L.D., Wang, M., Wang, D.L., Guo, Z.S. and Cao, F.C. (2007), "Flutter and buffeting performances of third Nanjing bridge over Yantze river under yaw wind via aeroelastic model test". *J. Wind Eng. Ind. Aerod.*, **95**(9-11), 1579-1606.
Zhu, L.D., Xu, Y.L., Zhang, F. and Xiang, H.F. (2002a), "Tsing Ma bridge deck under skew winds. Part Ⅰ: aerodynamic coefficients", *J. Wind Eng. Ind. Aerod.*, **90**(7), 782-805.
Zhu, L.D., Xu, Y.L. and Xiang, H.F. (2002b), "Tsing Ma bridge deck under skew winds-Part II: flutter derivatives", *J. Wind Eng. Ind. Aerod.*, **90**(7), 807-837.

JH